Potential Applications of PET Imaging in Developing Novel Cancer Therapies*

Roland Hustinx, Stephen L. Eck and Abass Alavi

Divisions of Nuclear Medicine and Hematology-Oncology, Hospital of the University of Pennsylvania, Philadelphia; and Institute for Human Gene Therapy, University of Pennsylvania, Philadelphia, Pennsylvania

Key Words: PET; gene therapy
J Nucl Med 1999; 40:995–1002

Gene therapy is one of the most promising new treatments for cancer. Clinical trials are under way in numerous centers for many malignant disorders, including phase I/II clinical trials for brain, breast, lung, colon and prostate cancers (*1–5*).

TRANSFERRING GENES INTO CANCER CELLS

Several approaches to gene therapy are being tested using a variety of vectors and therapeutic genes. However, all rely on the same rationale: genetically engineering a target tissue to produce a new therapeutic protein. This requires the selective introduction of genes into a target tissue (e.g., tumor cells) using a vector. Such vectors include adenovirus, retrovirus, adeno-associated virus, deoxyribonucleic acid (DNA)-protein complexes and liposomes (*6*). The vector has several roles: It packages the DNA gene of interest. It delivers the gene across the cell membrane and into the nucleus, and it drives expression of the gene to produce the therapeutic protein. Among others, three major approaches in cancer gene therapy have been extensively investigated (*1–5*).

1. Enzyme/prodrug systems, such as herpes simplex virus thymidine kinase/ganciclovir (HSV*tk*/GCV), that introduce a drug-activating enzyme.
2. Targeting aberrant molecular tumor cell pathways such as over-expression of wild-type p53 to arrest cell growth.
3. Introduction of proteins that stimulate the immune response to the tumor.

Received Feb. 2, 1999; revision accepted Mar. 5, 1999.
For correspondence or reprints contact: Abass Alavi, MD, Division of Nuclear Medicine, Hospital of the University of Pennsylvania, Donner Building, Rm. 110, 3400 Spruce St., Philadelphia, PA 19104.
*NOTE: FOR CE CREDIT, YOU CAN ACCESS THIS ARTICLE ON THE SNM WEB SITE (http://www.snm.org) UNTIL DECEMBER 1999.

The HSV*tk*/GCV Approach

The HSV*tk*/GCV system is one of the most widely investigated cancer gene therapy approaches and is also particularly well suited to the application of PET imaging. Phosphorylation by viral kinases (e.g., HSV*tk*) triggers the therapeutic effect of GCV, an acyclic nucleoside. HSV*tk* also phosphorylates related drugs (acyclovir, penciclovir and others) and is widely used to treat HSV and cytomegalovirus infections. In this setting, the viral thymidine kinase activates the drug to a monophosphate. Subsequent phosphorylation of the monophosphate compound by cellular kinases leads to inhibition of DNA synthesis (*7*). GCV is a poor substrate for the mammalian thymidine kinase, as shown by its low toxicity in humans.

This has been exploited in several recent cancer gene therapy trials (*8*). The HSV*tk* gene is delivered in a recombinant viral vector and is expressed only in tumor cells that are infected by the vector. The HSV*tk* protein in the tumor cells is able to phosphorylate intravenously administered GCV. As a result, these cells are selectively killed by the phosphorylated products of HSV*tk* (Fig. 1A). This process is further facilitated by intercellular communications (gap junctions) that allow the phosphorylated GCV to travel to adjacent tumor cells. This leads to the destruction of noninfected cells in the immediate vicinity (so-called "bystander effect") (*9*).

HSV*tk* cancer gene therapy was introduced by Moolten and Wells (*10*) and Moolten et al. (*11*) in animal models. Phase I clinical trials have shown encouraging results in treating tumors such as gliomas (*1,12*) and mesotheliomas (*13*). The phosphorylation of GCV by HSV*tk* (the rate-limiting step in drug activation) bears striking similarity to that of ^{18}F-fluorodeoxyglucose (FDG), a widely used PET tracer (Figs. 1B and C). Both require phosphorylation for substrate retention in the target tissue. FDG-6-phosphate accumulates in cells with increased glucose metabolism, including cancer cells. Therefore, tumors appear as foci of increased activity on PET images. Similarly, accumulation of phosphorylated derivatives of radiolabeled HSV*tk* substrates was predicted to provide images of tissues containing the HSV*tk* enzyme (i.e., tissues where gene expression was achieved).

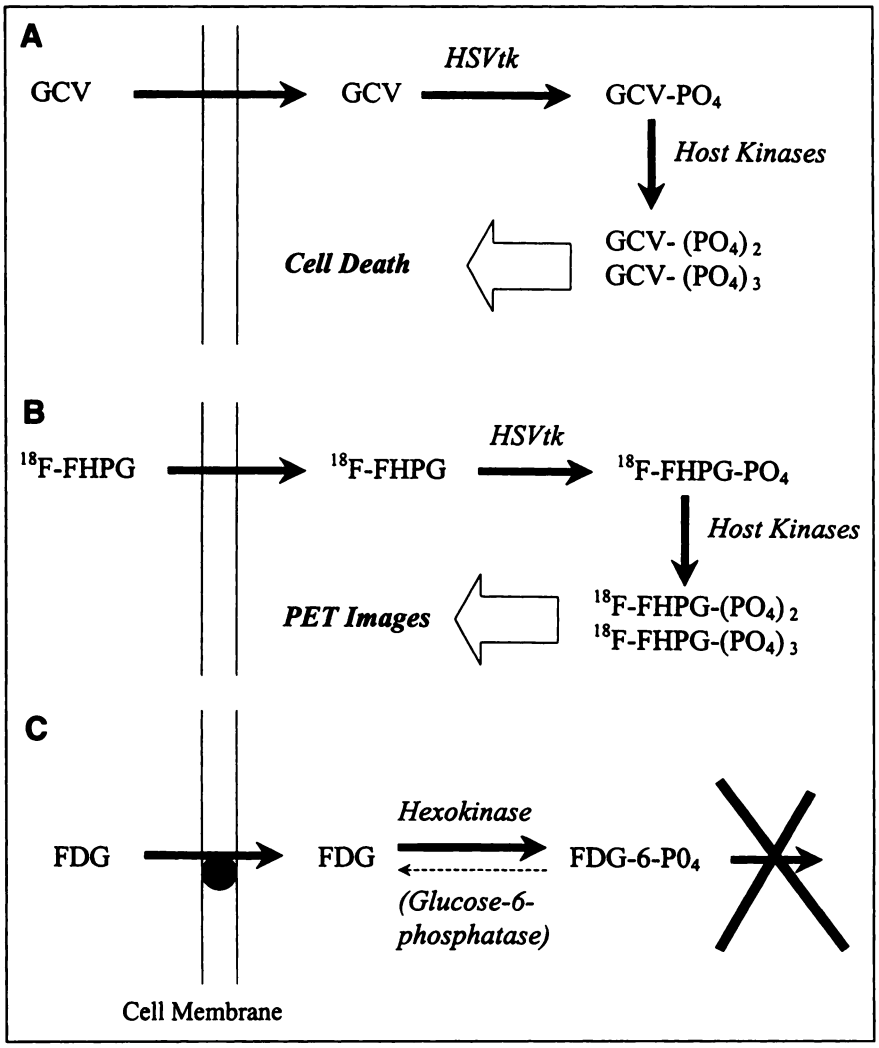

FIGURE 1. Mechanism of uptake of FDG and HSV*tk* substrates. FDG (C) and HSV*tk* substrates (as illustrated by GCV [A] and ^{18}F-FHPG [B]) accumulate in target cells as phosphorylated derivatives. There are significant differences between the two systems: enzyme catalyzing phosphorylation of FDG is endogenous, and its activity is enhanced in tumor cells, whereas nucleosides analogs are phosphorylated only after delivery of an exogenous therapeutic gene that mediates expression of enzyme. Increased expression of glucose membrane transporters enhances FDG uptake in tumor cells. In contrast, HSV*tk* substrates enter cells by passive diffusion with contributions from other transport mechanisms that vary with cell type. In addition, FDG-6-P0$_4$ is not a substrate for next enzyme of glucose metabolic pathway, whereas monophosphate products of HSV*tk* undergo further phosphorylation to di- and triphosphate derivatives.

Rationale for Assessing Gene Transfer

The major focus of cancer gene therapy is gene delivery to the target tissue, resulting in both protein expression and distribution within the tumor, in spite of any potential side effects that may be induced. Therefore, assessing the distribution and duration of the gene expression is of primary importance for evaluating new gene therapy approaches. Nuclear medicine techniques provide tremendous potential for improvement over current methods used to assess gene transfer.

Currently, biopsy specimens are obtained from the gene-treated tissues at specific times to determine gene transfer. This has several limitations, including sampling error, lack of information on distribution of gene transfer and significant risks and discomfort to the patient. The results of biopsy studies (when feasible) provide only limited data and typically cannot reliably assess the change in gene expression over time. Determining whether the gene therapy vector remains localized to the injection site or whether it becomes widely distributed throughout the tumor may have a great influence on the future design of vectors and clinical trials. For example, if reliable distribution data were available, the route and means of administration could be systematically varied so as to optimize tumor penetration by the vector. Finally, target tissue biopsies cannot reveal any information about unintended gene transfer into tissues that were not suspected of harboring the vector and, therefore, were not sampled. This is particularly important when considering the possibility of germline gene transfer (unintended gene delivery to testes or ovaries). Currently, the risk of germline gene transfer can be assessed only by inference from animal studies. Thus, there is a clear and compelling need for noninvasive, practical and sensitive methods for assessing gene transfer. The high sensitivity and specificity of radionuclide imaging may provide a solution to this problem.

PET TRACERS FOR ASSESSING HSV*tk* GENE TRANSFER AND EXPRESSION

Several radiotracers have been developed to image HSV*tk* expression in tumors (*14–19*). These are all substrates for HSV*tk* and are chemically derived from nucleosides used as therapeutic agents (Fig. 2).

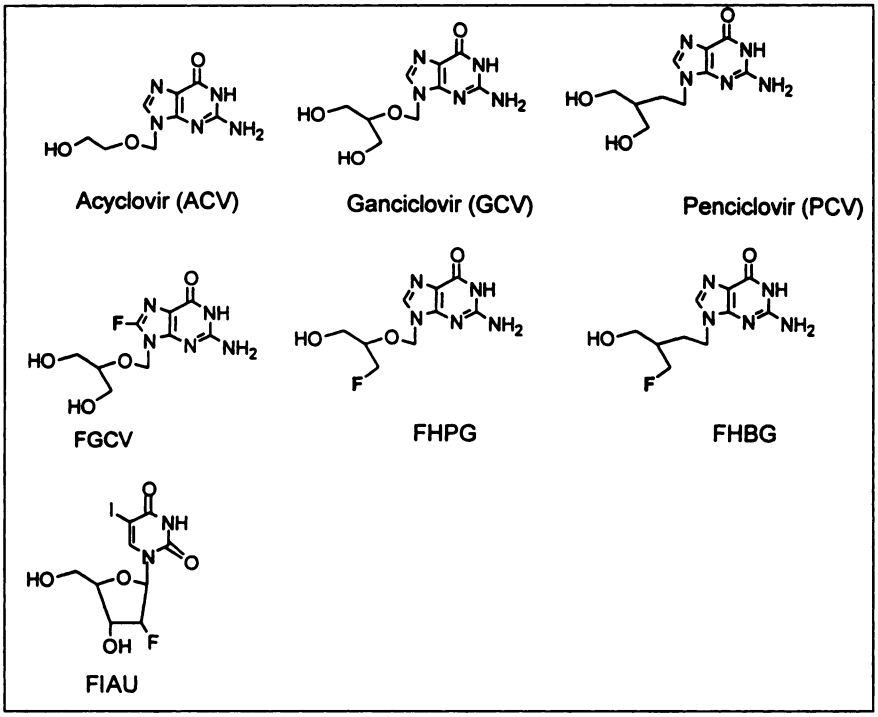

FIGURE 2. Chemical structures of substrates for HSV*tk*.

5-iodo-2′-fluoro-2′-deoxy-1-β-D-arabinofuranosyl-5-iodo-uracil

Tjuvajev et al. (*17*) have systematically developed 5-iodo-2′-fluoro-2′-deoxy-1-β-D-arabinofuranosyl-5-iodo-uracil (FIAU) as a tracer to monitor HSV*tk* gene therapy. They demonstrated that FIAU was a better substrate for HSV*tk* than was GCV. ^{131}I-FIAU was successfully used to image mammary and glial tumors that had been engineered to express HSV*tk* before inoculation into rats (*20*). Further studies with ^{124}I-FIAU produced high quality PET images of HSV*tk*-expressing mammary tumors in rats and demonstrated the high specificity of this agent for HSV*tk* expression. This was the first demonstration that HSV*tk*+ tumors could be successfully imaged with a positron-emitting radiopharmaceutical (*21*). Furthermore, a significant relationship was found between the level of tracer accumulation (% injected dose/g of tissue) and the level of expression of HSV*tk*. These results demonstrated the validity of the concept and encouraged the development of other applications using PET to detect and monitor gene expression.

The FIAU approach, however, is not without its limitations. The relatively long half-life of ^{124}I allows for delayed imaging (images can be acquired 36 h after injection) and thus increases the target-to-background contrast. However, from a practical point of view, a 1-d protocol that uses more specific radiotracers has several advantages, including early results (within hours) and the convenience for the patient of a single-day protocol. In addition, ^{124}I is available in only a limited number of sites, which further complicates the routine use of this approach.

[8-^{18}F]-fluoroganciclovir and 9-[(3-[^{18}F]-fluoro-1-hydroxy-2-propoxy) methyl]guanine

Administration of readily available short-lived radionuclides such as ^{18}F results in low radiation exposure. Also, the physical properties of ^{18}F are better suited than those of ^{124}I for quantitative PET imaging (*22*). Several radiolabeled GCV compounds have been developed over the past several years. GCV has been labeled with ^{18}F either on the 8 position of the acycloguanosine ring or on the 3 position of its side chain (Fig. 2).

[8-^{18}F]-fluoroganciclovir (^{18}F-FGCV) was first synthesized by Barrio et al. (*23*). Alauddin et al. (*15*) and Monclus et al. (*24,25*) developed the synthesis of 9-[(3-[^{18}F]-fluoro-1-hydroxy-2-propoxy)methyl]guanine (^{18}F-FHPG). Haberkorn et al. (*26,27*) performed a series of in vitro experiments to study the transport and metabolism of ^{3}H-GCV in various tumor cell lines. They showed significantly increased uptake of ^{3}H-GCV in the HSV*tk* transduced cells. This uptake was associated with a time-dependent phosphorylation of the compound. The uptake in wild-type cells (HSV*tk*−) was low, and only the unmetabolized ^{3}H-GCV was present in these cells. Moreover, ^{3}H-GCV uptake was strongly correlated with the percentage of HSV*tk*-expressing cells. This observation is of great significance because a small fraction of HSV*tk*+ cells can produce GCV phosphates that are exported to nearby cells.

After the administration of therapeutic doses of GCV, these nontransduced cells are killed as a result of their proximity to the transduced cells (bystander effect). In the in vivo situation, the distribution of the radiolabeled GCV uptake will therefore reflect tracer activity in the HSV*tk*+

cells and the surrounding cells that have secondarily acquired the phosphorylated tracer. However, in vivo, the spatial distribution and kinetics of the bystander effect are not well characterized; therefore, its contribution to the PET image is not yet known. Ideally, cancer gene therapists want to engineer approaches that have a large and rapid bystander effect (e.g., active drug is rapidly carried far beyond the tumor cells that express the therapeutic gene). In such a circumstance, the PET images would reflect the real extent of the distribution of active drug. If the bystander effect is small (as is likely the case with current HSV*tk* systems), then the PET images will, for all intents and purposes, reflect only the activity of the gene-expressing cells.

Recently, it has been shown that there is a strong correlation between labeled GCV uptake and the growth inhibition in response to pharmacological doses of GCV (*27*). These observations suggest that the uptake of radiolabeled GCV can be used not only as a marker of the presence and distribution of HSV*tk* in tumors but as a predictor of response to therapy. Although speculative at this time, such data obtained early in the course of GCV therapy (typically 10–14 d) might influence the dose or duration of GCV to be used to achieve the optimal therapeutic outcome.

In experiments more closely resembling a potential therapeutic application, Gambhir et al. (*28*) recently published images obtained using ^{18}F-FGCV in mice after in vivo gene transfer. Mice were treated intravenously with a recombinant adenovirus carrying HSV*tk* to effect HSV*tk* gene expression in the liver (primary site of adenovirus uptake after intravenous injection). The liver demonstrated increased activity on PET, which is consistent with retention of ^{18}F-FGCV-phosphates. Biodistribution studies showed relatively low levels of uptake in other organs, except for the urinary system, which reflected excretion of unmetabolized tracer. The same group also demonstrated the feasibility of using a three-compartment model to characterize the tracer kinetics in the same animal model (*29*). To date, there have been no reports studying tumor-bearing animals with ^{18}F-FGCV.

^{18}F-FHPG has been more extensively studied than other tracers. In vitro studies have shown high and selective accumulation of the tracer in various tumor cell types (*24*). Pharmacokinetic studies in monkeys have demonstrated acceptable radiation dosimetry for sensitive organs and the absence of recirculating labeled metabolites (*30*). In addition, the synthesis process has been simplified and shortened. Yields of 10%–15% are usually obtained in 1 h (*31*). We have studied this compound in glioma and mesothelioma tumor cell cultures with virus-delivered HSV*tk* (*32*) and found results comparable with those of other studies, i.e., *tk*+/*tk*− activity ratios ranging from 5 to 28 after 3 h of incubation with ^{18}F-FHPG. When the tracer was injected into mice 48 h after the intravenous administration of a recombinant adenovirus carrying the HSV*tk* gene, only liver and bladder activity was detected by PET imaging (Head PENN-PET scanner; UGM, Philadelphia, PA) (*32*). No hepatic uptake was seen in mice injected with a control adenovirus vector (Fig. 3). In rodents, HSV*tk*-expressing subcutaneous tumors (mesothelioma or glioma cell lines) were clearly visualized as early as 90 min post-tracer injection. Tumor-to-muscle activity ratios obtained by counting the tissues in a gamma well counter averaged 5.5 for HSV*tk*-expressing tumors, compared with 0.8 for control lesions. Expressed as percentage of dose per gram of tissue, these results were 3.4% and 0.6%, respectively. Tumor positivity by PET imaging correlated with the immunohistochemical staining of the tissues using monoclonal antibodies directed against HSV*tk* protein (*13*).

Recently, labeling methodology for penciclovir (PCV) 9-(4-hydroxy-3-hydroxymethylbutyl)guanine with ^{18}F was reported (Fig. 2) (*33*). Compared with GCV, PCV has a higher phosphorylation rate by viral thymidine kinase, greater intracellular stability of its phosphorylated form and more effective inhibition of the DNA polymerase (*34,35*). The higher rate of phosphorylation of PCV is important for PET imaging. Preliminary in vitro studies comparing PCV and GCV in colon adenocarcinoma and glioma cell lines have shown higher accumulation of PCV labeled either with ^{3}H on the 8 position of the ring (*36*) or with ^{18}F on the 3 position of the side chain (*33*).

Other nucleosides such as 5-fluoro-1-(2′-deoxy-2′-fluoro-β-D-ribofuranosyl)uracil (FFUdR) can be labeled with ^{18}F (*37*). In vitro experiments have shown higher uptake of FFUdR than GCV in HSV*tk*-transduced hepatoma cells, but this was also true in control cells, because FFUdR is also phosphorylated by the mammalian thymidine kinase (*19*). This is likely to increase the background activity during in vivo imaging; however, a side-by-side comparison of the tracers remains to be done.

FDG PET imaging has also been tested as a means for

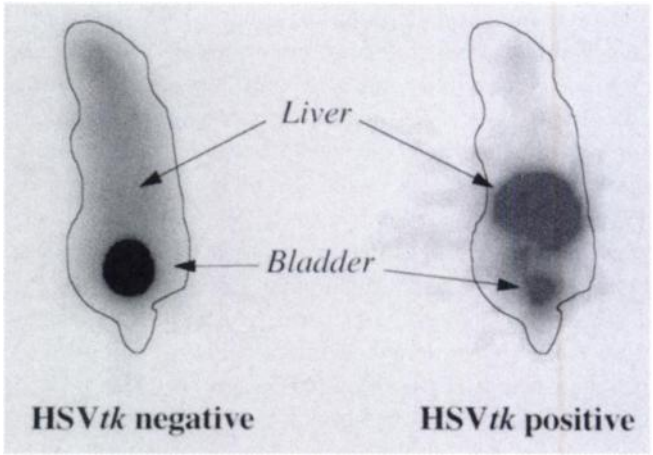

FIGURE 3. Coronal PET images obtained 2 h after intravenous injection of ^{18}F-FHPG into two mice. Forty-eight hours before imaging, mouse A was injected intravenously with control vector, whereas mouse B received recombinant adenovirus carrying HSV*tk*. In HSV*tk*-treated animal, tracer specifically concentrates in liver, which is primary site of adenovirus uptake after intravenous injection. Only uptake seen in control animal is in bladder.

monitoring the effects of gene therapy. Haberkorn et al. (*38*) found an uncoupling of FDG transport and phosphorylation in rat hepatomas during gene therapy with HSV*tk* and GCV. After 2 d of treatment, FDG transport was enhanced, yet phosphorylation remained unaffected. After 4 d, transport normalized, although phosphorylation increased. Initial increased transport was interpreted as a reaction to cellular stress, whereas the therapeutic effects leading to cell death explain the later decline. The increased phosphorylation rate was observed in vivo but not in previous in vitro experiments conducted by the same researchers (*39*). These observations may have a significant influence on FDG PET imaging in patients who are treated with such protocols, with respect to the timing of the studies.

ASSESSMENT OF TUMOR HYPOXIA

Tumor hypoxia is an important factor that limits response to radiation in animal models as well as in human cancers (*40*). Radiation therapy is not the only treatment modality influenced by tumor hypoxia. Hypoxic tumor cells, because of their relative isolation from blood supply or free-radical-based mechanism of toxicity, are also resistant to some cytotoxic drugs (*41*). In addition, studies have demonstrated the importance of hypoxia in patients who are treated surgically. For example, pretreatment hypoxia was associated with a higher rate of locoregional recurrence of carcinoma of the cervix (*42*). Poor outcome from distant metastases has also been demonstrated in hypoxic soft-tissue sarcomas treated by multimodality therapy (*43*). Tissue hypoxia exists in a substantial proportion of tumors, although it varies with tumor type, among patients and within lesions in a single patient (*44–46*). Recurrent tumors may also have a different oxygenation state than the primary lesion (*47*).

Current Limitations

In patients, tumor hypoxia is currently measured using the Eppendorf oxygen microelectrode, which can directly measure oxygen tension in tissues. Eppendorf studies have shown a high degree of heterogeneity in human tumors of otherwise similar characteristics. This heterogeneity has been found in all tumor types examined (*48,49*). The sensitivity and specificity of this method are suboptimal, because interobserver variability is high and the results are operator-dependent (*50*). Although it can be performed intraoperatively, the technique is usually limited to superficially accessible tumors. Multiple assays are necessary to determine the degree of oxygenation of the entire tumor. Nonetheless, the method is still prone to sampling errors. Finally, because necrotic parts of the tumor are read as hypoxic, Eppendorf studies have a tendency to overestimate the hypoxic fraction of the viable tumor. Recently, immunohistochemical staining for pimonidazole (a 2-nitroimidazole) binding on tumor tissue was introduced as a measure of hypoxia (*51*). Tissue samples are obtained by multiple-punch biopsies 24 h after intravenous administration of pimonidazole. By combining immunohistochemical assays for endogenous proliferation markers with immunostaining for pimonidazole, tumor hypoxia can be compared with other physiological parameters of tumor growth.

Imidazole Derivatives and PET

Imidazole derivatives are bio-reductively activated drugs with well-known radiosensitizing, cytotoxic and metabolic properties (*52,53*). The reductive metabolism of these compounds leads to their activation and subsequent formation of covalent bonds with cellular molecules under hypoxic conditions. This process is gradually inhibited as oxygen concentration increases (*54*). Several ^{18}F-labeled compounds (^{18}F-fluoromisonidazole [FMISO], ^{18}F-fluoroerythronitroimidazole [FETNIM], ^{18}F-fluoroetanidazole) have been synthesized, to take advantage of both the biochemical properties of imidazole derivatives and the high resolution of PET (*55–57*). Among these tracers, ^{18}F-FMISO has been most extensively studied (Fig. 4). ^{18}F-FMISO PET imaging was successfully used to evaluate the presence of tumor hypoxia before treatment (*55,56,58*) or during fractionated irradiation (*59*). Although quantitative values can be obtained through compartmental analysis (*60*), simple methods can be used for practical application of this method. Measurement of the fractional hypoxic volume (proportion of pixels in the tumor volume with a tissue-to-blood activity $\geq$1.4 at 120 min postinjection) (*56*) or the tumor-to-muscle retention ratio (*61*) appears to be useful for detecting tumor hypoxia. Despite these encouraging preliminary results, suboptimal imaging properties (low target-to-background ratio, slow uptake in the tumor) have limited the use of ^{18}F-FMISO in routine clinical practice. Other imidazole derivatives have been developed. In tumor-bearing rats, ^{18}F-FETNIM displayed higher tumor-to-blood activity ratios than FMISO (*57*), but no subsequent studies have confirmed this early observation. Recently, the synthesis of ^{18}F-fluoroetanidazole was reported (*62*), but no data are available about the in vivo properties of this compound.

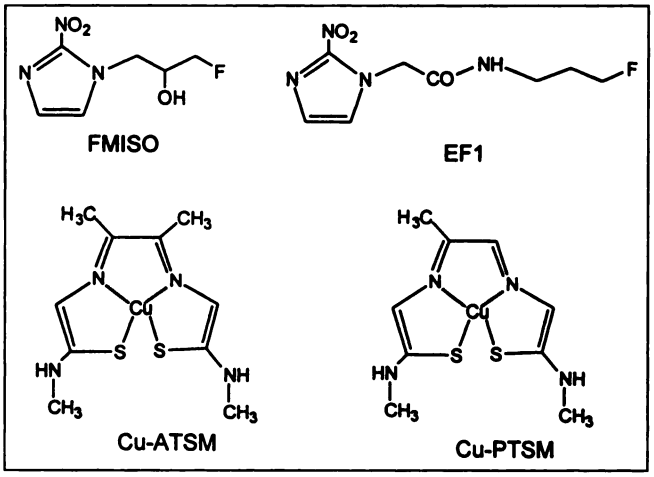

FIGURE 4. Chemical structures of compounds investigated for their hypoxia-detecting properties.

The 2-nitroimidazole, EF5, has been studied extensively using immunohistochemical technique for the detection of the reduced adducts in tissues. Correlation of EF5 binding to several independent endpoints, including radiation response and tumor red blood cell flux, has been made (*63,64*). A.V. Kachur et al. have developed the ^{18}F-labeled PET imaging agent of a sister drug to EF5 called [F-18]-N-(3-monofluoropropyl)-2-(2-nitroimidazol-1[H]-yl)-acetamide (^{18}F-EF1) (Fig. 4) (unpublished data, 1999). Both EF1 and EF5 are similar in structure to etanidazole, which is the least toxic 2-nitroimidazole studied in humans. Both are much more stable in vivo than is misonidazole. About 70% of the injected dose is excreted in the urine in unaltered forms, compared with less than 10% for misonidazole (*65*). In addition, its hypoxia-dependent metabolism is much more predictable than that of misonidazole and other compounds.

We have performed PET imaging with ^{18}F-EF1 in tumor-bearing rats (unpublished data). Biodistribution studies showed that the tracer was excreted primarily by the urinary tract. Hypoxic tumors (Q7 hepatomas) showed tumor-to-muscle activity ratios of 2.7 and 2.4 at 150 min postinjection. For normoxic tumors (9LF gliomas), these values were 0.8 and 0.5, respectively. These results correlated well with the oxygenation status of the tumors, which was measured with an independent method. Immunohistochemical detection of intracellular EF3 using a monoclonal antibody for assessment of tumor hypoxia in tissue samples is well validated (*66,67*) and was performed in all the animals.

Radiolabeling of the multifluorinated EF5 would certainly improve the imaging characteristics of the compound. Its greater lipophilicity would allow for an easier penetration through the cell membranes and the blood-brain barrier. This property, combined with the high hypoxia selectivity of the compound and its predominant urinary excretion, would provide a high target-to-background ratio relatively soon after injection of the tracer. EF5 is currently being tested as a diagnostic agent for hypoxia in human tumors; thus far, no adverse events have been observed (Evans SM, personal communication).

Copper-Labeled Thiosemicarbazone Complexes and PET

A radically different approach has been followed by other groups who have used copper (either ^{62}Cu or ^{64}Cu)-labeled compounds (Fig. 4). ^{62}Cu-pyruvaldehyde-bis(N4-methylthiosemicarbazone) (PTSM), a bis(thiosemicarbazone) (BTS) derivative, is a well-known perfusion tracer. Incidentally, retention in rat brain after transient ischemia has been reported (*68*). ^{62}Cu-diacetyl-bis(N4-methylthiosemicarbazone) (ATSM), another Cu-BTS complex, was not significantly taken up by normoxic rat heart, whereas in hypoxic conditions, the uptake was markedly increased (*69*). Preliminary results in PET studies were reported with ^{62}Cu-ATSM in lung cancer patients, showing high tumor-to-background contrast compared with minimal uptake in the lungs of normal subjects (*70*). The oxygen concentration of these tumors was not independently assessed, but studies by the same group suggest that retention in tumor cells primarily depends on a cytosolic/microsomal bioreduction, in particular nicotinamide adenine dinucleotide hydroxide (NADH)-cytochrome P450 reductase and NADH-cytochrome b5 reductase (*71*).

These enzymes are also responsible for the hypoxic activation of bioreductive drugs. Dearling et al. (*72*) have tested various ^{64}Cu-labeled BTS complexes and found high hypoxia selectivity in several of such compounds. Recently, Lewis et al. (*73*) compared the uptake of ^{64}Cu-ATSM, ^{64}Cu-PTSM and ^{18}F-FMISO in tumor cells under various oxygen concentrations. Both ^{64}Cu-ATSM and ^{18}F-FMISO showed oxygen concentration-dependent uptake. However, ^{64}Cu-ATSM uptake was significantly higher than that of ^{18}F-FMISO. ^{64}Cu-PTSM uptake did not vary with the oxygen concentration. Biodistribution studies showed that the uptake in the tumor peaked as early as 10 min postinjection. There was also significant uptake in the lungs, and the tracer was excreted through the liver and kidneys. Autoradiographic studies showed heterogeneous uptake of ^{64}Cu-ATSM in the tumors, in contrast with the homogeneous distribution of ^{64}Cu-PTSM (reflecting the blood flow). These results suggest that ^{64}Cu-ATSM is selectively and rapidly taken up by hypoxic tumors.

Several issues remain to be addressed: in particular, the biodistribution and pharmacokinetics of such compounds. Liver uptake is followed by bowel excretion, which could generate abdominal activity on the images. In addition, washout from most of the organs appears to be slow, and there is limited information about the muscle uptake. Therefore, it is not yet known whether the in vivo target-to-background ratio will allow appropriate imaging. However, this approach, although still in its infancy, is attractive, and these tracers warrant further investigation.

CONCLUSION

Although the first attempts to assess tumor hypoxia with nuclear medicine techniques were performed in the 1980s, recent advances have shown continued promise. In particular, development of 2-nitroimidazole tracers with excellent imaging properties and initial studies with copper-labeled compounds are encouraging. A noninvasive and routinely applicable imaging method could provide valuable information regarding the role of tumor hypoxia in the natural history of cancers and their response to therapy. Similarly, by developing radiotracers that are specific to the engineered gene product, nuclear medicine has the potential to play a significant role in the evaluation of experimental gene therapy strategies. In particular, it may bridge the gap between experimental animal models and human applications by providing valuable information regarding the distribution and duration of gene expression.

ACKNOWLEDGMENTS

The authors thank Sydney M. Evans, VMD, and Cameron C. Koch, PhD, for reviewing the manuscript and Uwe

Haberkorn, MD, for fruitful discussions. This work was supported by funds from the National Institutes of Health/ National Cancer Institute (PO1 CA66726, P30 CA16520, PO1 CA67790), pilot research grants from the Society of Nuclear Medicine. Support was also provided by a scientific research grant from the North Atlantic Treaty Organization and by the "Fondation Medicale M.E. Horlais-Dapsens."

REFERENCES

1. Alavi JB, Eck SL. Gene therapy for malignant gliomas. *Hematol Oncol Clin North Am.* 1998;12:617–629.
2. Boxhorn HKE, Eck SL. Gene therapy for breast cancer. *Hematol Oncol Clin North Am.* 1998;12:665–675.
3. Dubinett SM, Miller PW, Sharma S, Batra RK. Gene therapy for lung cancer. *Hematol Oncol Clin North Am.* 1998;12:569–594.
4. Zwacka RM, Dunlop MG. Gene therapy for colon cancer. *Hematol Oncol Clin North Am.* 1998;12:595–615.
5. Malkowicz SB, Johnson JO. Gene therapy for prostate cancer. *Hematol Oncol Clin North Am.* 1998;12:649–664.
6. Dranoff G. Cancer gene therapy: connecting basic research with clinical inquiry. *J Clin Oncol.* 1998;16:2548–2556.
7. Matthews T, Boehme R. Antiviral activity and mechanism of action of anciclovir. *Rev Infect Dis.* 1988;10:S490–S494.
8. Ram Z, Culver KW, Oshiro EM, et al. Therapy of malignant brain tumors by intratumoral implantation of retroviral vector-producing cells. *Nat Med.* 1997;3: 1354–1361.
9. Yang L, Chiang Y, Lenz HJ, et al. Intercellular communication mediates the bystander effect during herpes simplex thymidine kinase/ganciclovir-based gene therapy of human gastrointestinal tumor cells. *Hum Gene Ther.* 1998;9:719–728.
10. Moolten FL, Wells JM. Curability of tumors bearing herpes thymidine kinase genes transferred by retroviral vectors. *J Natl Cancer Inst.* 1990;82:297–300.
11. Moolten FL, Wells JM, Heyman RA, Evans RM. Lymphoma regression induced by ganciclovir in mice bearing a herpes thymidine kinase transgene. *Hum Gene Ther.* 1990;1:125–134.
12. Eck SL, Alavi JB, Alavi A, et al. Treatment of advanced CNS malignancies with the recombinant adenovirus H5.010RSVTK: a phase I trial. *Hum Gene Ther.* 1996;7:1465–1482.
13. Sterman DH, Treat J, Litzky LA, et al. Adenovirus-mediated herpes simplex virus thymidine kinase/ganciclovir gene therapy in patients with localized malignancy: results of a phase I clinical trial in malignant mesothelioma. *Hum Gene Ther.* 1998;9:1083–1092.
14. Monclus M, Luxen A, Van Naemen J, et al. Development of PET radiopharmaceuticals for gene therapy: synthesis of 9-((1-(^{18}F)fluoro-3-hydroxy-2-propoxy)methyl)guanine. *J Labelled Compd Radiopharm.* 1995;37:193–195.
15. Alauddin MM, Conti PS, Mazza SM, Hamzeh FM, Lever JR. 9-[(3-[^{18}F]-fluoro-1-hydroxy-2-propoxy)methyl]guanine ([^{18}F]-FHPG): a potential imaging agent of viral infection and gene therapy using PET. *Nucl Med Biol.* 1996;23:787–792.
16. Barrio JR, Namavari M, Satyamurthy N, et al. 8-(F-18)fluoroacyclovir: an in-vivo probe for gene expression with PET [abstract]. *J Nucl Med.* 1996;37:193P–194P.
17. Tjuvajev JG, Stockhammer G, Desai R, et al. Imaging the expression of transfected genes in vivo. *Cancer Res.* 1995;55:6126–6132.
18. Morin KW, Knaus EE, Wiebe LI. Non-invasive scintigraphic monitoring of gene expression in a HSV-1 thymidine kinase gene therapy model. *Nucl Med Commun.* 1997;18:599–605.
19. Germann C, Shields AF, Grierson JR, Morr I, Haberkorn U. 5-Fluoro-1-(2′-deoxy-2′-fluoro-beta-D-ribofuranosyl) uracil trapping in Morris hepatoma cells expressing the herpes simplex virus thymidine kinase gene. *J Nucl Med.* 1998;39:1418–1423.
20. Tjuvajev JG, Finn R, Watanabe K, et al. Noninvasive imaging of herpes virus thymidine kinase gene transfer and expression: a potential method for monitoring clinical gene therapy. *Cancer Res.* 1996;56:4087–4095.
21. Tjuvajev JG, Avril N, Oku T, et al. Imaging herpes virus thymidine kinase gene transfer and expression by positron emission tomography. *Cancer Res.* 1998;58: 4333–4341.
22. Pentlow KS, Graham MC, Lambrecht RM, et al. Quantitative imaging of iodine-124 with PET. *J Nucl Med.* 1996;37:1557–1562.
23. Barrio JR, Namavari M, Srinivasan A, et al. Carbon-8 radiofluorination of purines: a general approach to probe design for gene therapy in humans. *J Labelled Compd Radiopharm.* 1997;40:348.
24. Monclus M, Luxen A, Cool V, Damhaut P, Velu T, Goldman S. Development of a positron emission tomography radiopharmaceutical for imaging thymidine kinase gene expression: synthesis and in vitro evaluation of 9-((3-(^{18}F)fluoro-1-hydroxy-2-propoxy)methyl)guanine. *Bioorg Med Chem.* 1997;7:1879–1882.
25. Monclus M, Luxen A, Cool V, et al. Synthesis of (R)- and (S)-9-((3-(^{18}F)fluoro-1-hydroxy-2-propoxy)methyl)guanine: radiopharmaceuticals for gene therapy. *J Labelled Compd Radiopharm.* 1997;40:20–22.
26. Haberkorn U, Altmann A, Morr I, et al. Monitoring gene therapy with herpes simplex virus thymidine kinase in hepatoma cells: uptake of specific substrates. *J Nucl Med.* 1997;38:287–294.
27. Haberkorn U, Khazaie K, Morr I, Altmann A, Muller M, van Kaick G. Ganciclovir uptake in human mammary carcinoma cells expressing herpes simplex virus thymidine kinase. *Nucl Med Biol.* 1998;25:367–373.
28. Gambhir SS, Barrio JR, Wu L, et al. Imaging of adenoviral-directed herpes simplex virus type 1 thymidine kinase reporter gene expression in mice with radiolabeled ganciclovir. *J Nucl Med.* 1998;39:2003–2011.
29. Green LA, Gambhir SS, Barrio JR, et al. Tracer kinetic modeling of 8-(F-18)-fluoroganciclovir PET data: a new tracer for measuring reporter gene expression [abstract]. *J Nucl Med.* 1998;39:10P.
30. Bading JR, Alauddin MM, Fissekis JH, Kirkman E, Raman RK, Conti PS. Pharmacokinetics of F-18 fluorohydroxy-propoxymethylguanine (FHPG) in primates [abstract]. *J Nucl Med.* 1997;38:43P.
31. Shiue CY, Shiue GG, McDonald D, Eck S, Alavi AA. Simplified one-pot synthesis of 9-((3-(F-18)fluoro-1-hydroxy-2-propoxy)methyl)guanine ((F-18)FHPG,2) for gene therapy [abstract]. *J Nucl Med.* 1998;39:231P.
32. Karp JS, Freifelder R, Geagan MJ, et al. Three-dimensional imaging characteristics of the HEAD PENN-PET scanner. *J Nucl Med.* 1997;38:636–643.
33. Alauddin MM, Conti PS. Synthesis and preliminary evaluation of 9-(4-[^{18}F]-fluoro-3-hydroxymethylbutyl)guanine ([^{18}F]FHBG): a new potential imaging agent for viral infection and gene therapy using PET. *Nucl Med Biol.* 1998;25:175–180.
34. Earnshaw DL, Bacon TH, Darlison SJ, Edmonds K, Perkins RM, Vere Hodge RA. Mode of antiviral action of penciclovir in MRC-5 cells infected with herpes simplex virus type 1 (HSV-1), HSV-2, and varicella-zoster virus. *Antimicrob Agents Chemother.* 1992;36:2747–2757.
35. Smee DF, Boehme R, Chernow M, Binko BP, Matthews TR. Intracellular metabolism and enzymatic phosphorylation of 9-(1,3-dihydroxy-2-propoxymethyl)guanine and acyclovir in herpes simplex virus-infected and uninfected cells. *Biochem Pharmacol.* 1985;34:1049–1056.
36. Gambhir SS, Barrio JR, Bauer E, et al. Radiolabeled penciclovir: a new reporter probe with improved imaging properties over ganciclovir for imaging herpes-simplex virus type 1 thymidine kinase reporter gene expression [abstract]. *J Nucl Med.* 1998;39:53P.
37. Shields AF, Grierson JR, Kozawa SM, Zheng M. Development of labeled thymidine analogs for imaging tumor proliferation. *Nucl Med Biol.* 1996;23: 17–22.
38. Haberkorn U, Belleman ME, Gerlach L, et al. Uncoupling of 2-fluoro-2-deoxyglucose transport and phosphorylation in rat hepatoma during gene therapy with HSV thymidine kinase. *Gene Ther.* 1998;5:880–887.
39. Haberkorn U, Altmann A, Morr I, Germann C, Oberdorfer F, van Kaick G. Multitracer studies during gene therapy of hepatoma cells with herpes simplex virus thymidine kinase and ganciclovir. *J Nucl Med.* 1997;38:1048–1054.
40. Moulder JE, Rockwell S. Hypoxic fractions of solid tumors: experimental techniques, methods of analysis, and a survey of existing data. *Int J Radiat Oncol Biol Phys.* 1984;10:695–712.
41. Adams GE. Hypoxia-mediated drugs for radiation and chemotherapy. *Cancer.* 1981;48:696–707.
42. Hockel M, Knoop C, Schlenger K, et al. Intratumoral pO_2 predicts survival in advanced cancer of the uterine cervix. *Radiother Oncol.* 1993;26:45–50.
43. Brizel DM, Scully SP, Harrelson JM, et al. Tumor oxygenation predicts for the likelihood of distant metastases in human soft tissue sarcoma. *Cancer Res.* 1996;56:941–943.
44. Gatenby RA, Kessler HB, Rosenblum JS, et al. Oxygen distribution in squamous cell carcinoma metastases and its relationship to outcome of radiation therapy. *Int J Radiat Oncol Biol Phys.* 1988;14:831–838.
45. Hockel M, Schlenger K, Knoop C, Vaupel P. Oxygenation of carcinomas of the uterine cervix: evaluation by computerized O_2 tension measurements. *Cancer Res.* 1991;51:6098–6102.
46. Hockel M, Schlenger K, Aral B, Mitze M, Schaffer U, Vaupel P. Association between tumor hypoxia and malignant progression in advanced cancer of the uterine cervix. *Cancer Res.* 1996;56:4509–4515.
47. Hockel M, Schlenger K, Hockel S, Aral B, Schaffer U, Vaupel P. Tumor hypoxia in pelvic recurrences of cervical cancer. *Int J Cancer.* 1998;79:365–369.
48. Rampling R, Cruickshank G, Lewis AD, Fitzsimmons SA, Workman P. Direct measurement of pO_2 distribution and bioreductive enzymes in human malignant brain tumors. *Int J Radiat Oncol Biol Phys.* 1994;29:427–431.

49. Brizel DM, Rosner GL, Harrelson J, Prosnitz LR, Dewhirst MW. Pretreatment oxygenation profiles of human soft tissue sarcomas. *Int J Radiat Oncol Biol Phys.* 1994;30:635–642.
50. Nozue M, Lee I, Yuan F, et al. Interlaboratory variation in oxygen tension measurement by Eppendorf "histograph" and comparison with hypoxic marker. *J Surg Oncol.* 1997;66:30–38.
51. Kennedy AS, Raleigh JA, Perez GM, et al. Proliferation and hypoxia in human squamous cell carcinoma of the cervix: first report of combined immunohistochemical assays. *Int J Radiat Oncol Biol Phys.* 1997;37:897–905.
52. Bremner JC, Stratford IJ, Bowler J, Adams GE. Bioreductive drugs and the selective induction of tumour hypoxia. *Br J Cancer.* 1990;61:717–721.
53. Cole S, Stratford IJ, Adams GE, Fielden EM, Jenkins TC. Dual-function 2-nitroimidazoles as hypoxic cell radiosensitizers and bioreductive cytotoxins: in vivo evaluation in KHT murine sarcomas. *Radiat Res.* 1990;124:S38–S43.
54. Chapman JD. The detection and measurement of hypoxic cells in solid tumors. *Cancer.* 1984;54:2441–2449.
55. Koh WJ, Rasey JS, Evans ML, et al. Imaging of hypoxia in human tumors with [F-18]fluoromisonidazole. *Int J Radiat Oncol Biol Phys.* 1992;22:199–212.
56. Rasey JS, Koh WJ, Evans ML, et al. Quantifying regional hypoxia in human tumors with positron emission tomography of [^{18}F]fluoromisonidazole: a pretherapy study of 37 patients. *Int J Radiat Oncol Biol Phys.* 1996;36:417–428.
57. Yang DJ, Wallace S, Cherif A, et al. Development of F-18-labeled fluoroerythronitroimidazole as a PET agent for imaging tumor hypoxia. *Radiology.* 1995;194: 795–800.
58. Valk P, Mathis C, Prados M, Gilbert J, Budinger T. Hypoxia in human gliomas: demonstration by PET with fluorine-18-fluoromisonidazole. *J Nucl Med.* 1992;33: 2133–2137.
59. Koh WJ, Bergman KS, Rasey JS, et al. Evaluation of oxygenation status during fractionated radiotherapy in human nonsmall cell lung cancers using [F-18]fluoromisonidazole positron emission tomography. *Int J Radiat Oncol Biol Phys.* 1995;33:391–398.
60. Casciari JJ, Graham MM, Rasey JS. A modeling approach for quantifying tumor hypoxia with [F-18]fluoromisonidazole PET time-activity data. *Med Phys.* 1995;22:1127–1139.
61. Yeh SH, Liu RS, Wu LC, et al. Fluorine-18 fluoromisonidazole tumour to muscle retention ratio for the detection of hypoxia in nasopharyngeal carcinoma. *Eur J Nucl Med.* 1996;23:1378–1383.
62. Tewson TJ. Synthesis of [^{18}F]fluoroetanidazole: a potential new tracer for imaging hypoxia. *Nucl Med Biol.* 1997;24:755–760.
63. Evans SM, Jenkins WT, Joiner B, Lord EM, Koch CJ. 2-Nitroimidazole (EF5) binding predicts radiation resistance in individual 9L s.c. tumors. *Cancer Res.* 1996;56:405–411.
64. Evans SM, Koch CJ, Laughlin KM, Jenkins WT, Van Winkle T, Wilson DF. Tamoxifen induces hypoxia in MCF-7 xenografts. *Cancer Res.* 1997;57:5155–5161.
65. Laughlin KM, Evans SM, Jenkins WT, et al. Biodistribution of the nitroimidazole EF5 (2-[2-nitro-1H-imidazol-1-yl]-N-(2,2,3,3,3-pentafluoropropyl) acetamide) in mice bearing subcutaneous EMT6 tumors. *J Pharmacol Exp Ther.* 1996;277:1049–1057.
66. Evans SM, Joiner B, Jenkins WT, Laughlin KM, Lord EM, Koch CJ. Identification of hypoxia in cells and tissues of epigastric 9L rat glioma using EF5 [2-(2-nitro-1H-imidazol-1-yl)-N-(2,2,3,3,3-pentafluoropropyl) acetamide]. *Br J Cancer.* 1995;72:875–882.
67. Lord EM, Harwell L, Koch CJ. Detection of hypoxic cells by monoclonal antibody recognizing 2-nitroimidazole adducts. *Cancer Res.* 1993;53:5721–5726.
68. Taniuchi H, Fujibayashi Y, Yonekura Y, Konishi J, Yokoyama A. Hyperfixation of copper-62-PTSM in rat brain after transient global ischemia. *J Nucl Med.* 1997;38:1130–1134.
69. Fujibayashi Y, Taniuchi H, Yonekura Y, Ohtani H, Konishi J, Yokoyama A. Copper-62-ATSM: a new hypoxia imaging agent with high membrane permeability and low redox potential. *J Nucl Med.* 1997;38:1155–1160.
70. Takahashi N, Fujibayashi Y, Yonekura Y, et al. Evaluation of copper-62 ATSM in patients with lung cancer as a hypoxic tissue tracer [abstract]. *J Nucl Med.* 1998;39:53P.
71. Fujibayashi Y, Yoshimi E, Waki A, Takahashi N, Yonekura Y. Cu-ATSM, a new tumor agent predicting ability for bioreductive drug activation [abstract]. *J Nucl Med.* 1998;39:90P.
72. Dearling JL, Lewis JS, Mullen GE, Rae MT, Zweit J, Blower PJ. Design of hypoxia-targeting radiopharmaceuticals: selective uptake of copper-64 complexes in hypoxic cells in vitro. *Eur J Nucl Med.* 1998;25:788–792.
73. Lewis JS, McCarthy DW, McCarthy TJ, Fujibayashi Y, Welch MJ. Evaluation of Cu-64-ATSM in vitro and in vivo in a hypoxic model. *J Nucl Med.* 1999;40:177–183.